Calcified Tissue International (2018) 103:443–454
https://doi.org/10.1007/s00223-018-0439-8

ORIGINAL RESEARCH

# Sclerostin Antibody Reverses the Severe Sublesional Bone Loss in Rats After Chronic Spinal Cord Injury

**Wei Zhao[1,2] · Xiaodong Li[5] · Yuanzhen Peng[1] · Yiwen Qin[1] · Jiangping Pan[1] · Jiliang Li[6] · Aihua Xu[6] · Michael S. Ominsky[5,9] · Christopher Cardozo[1,2,3] · Jian Q. Feng[7] · Hua Zhu Ke[8] · William A. Bauman[1,2,4] · Weiping Qin[1,2]**

Received: 16 November 2017 / Accepted: 8 May 2018 / Published online: 21 June 2018


## Abstract

To date, no efficacious therapy exists that will prevent or treat the severe osteoporosis in individuals with neurologically motor-complete spinal cord injury (SCI). Recent preclinical studies have demonstrated that sclerostin antibody (Scl-Ab) can prevent sublesional bone loss after acute SCI in rats. However, it remains unknown whether sclerostin inhibition reverses substantial bone loss in the vast majority of the SCI population who have been injured for several years. This preclinical study tested the efficacy of Scl-Ab to reverse the bone loss that has occurred in a rodent model after chronic motor-complete SCI. Male Wistar rats underwent either complete spinal cord transection or only laminectomy. Twelve weeks after SCI, the rats were treated with Scl-Ab at 25 mg/kg/week or vehicle for 8 weeks. In the SCI group that did not receive Scl-Ab, 20 weeks of SCI resulted in a significant reduction of bone mineral density (BMD) and estimated bone strength, and deterioration of bone structure at the distal femoral metaphysis. Treatment with Scl-Ab largely restored BMD, bone structure, and bone mechanical strength. Histomorphometric analysis showed that Scl-Ab increased bone formation in animals with chronic SCI. In ex vivo cultures of bone marrow cells, Scl-Ab inhibited osteoclastogenesis, and promoted osteoblastogenesis accompanied by increased Tcf7, ENC1, and the OPG/RANKL ratio expression, and decreased SOST expression. Our findings demonstrate for the first time that Scl-Ab reverses the sublesional bone loss when therapy is begun after relatively prolonged spinal cord transection. The study suggests that, in addition to being a treatment option to prevent bone loss after acute SCI, sclerostin antagonism may be a valid clinical approach to reverse the severe bone loss that invariably occurs in patients with chronic SCI.

**Keywords** Spinal cord injury · Sclerostin · Bone formation · Bone mineral density · Trabecular bone volume

## Abbreviations

| | |
|---|---|
| SCI | Spinal cord injury |
| *SOST* | Sclerostin |
| Scl-Ab | Sclerostin antibody |
| BMD | Bone mineral density |

**Electronic supplementary material** The online version of this article (https://doi.org/10.1007/s00223-018-0439-8) contains supplementary material, which is available to authorized users.

✉ Weiping Qin
weiping.qin@mssm.edu; weiping.qin@va.gov

1 National Center for the Medical Consequences of Spinal Cord Injury, James J. Peters VA Medical Center, 130 West Kingsbridge Road, Bronx, NY 10468, USA

2 Department of Medicine, Icahn School of Medicine at Mount Sinai, New York, NY, USA

3 Pharmacology and Systems Therapeutics, Icahn School of Medicine at Mount Sinai, New York, NY, USA

4 Rehabilitation Medicine, Icahn School of Medicine at Mount Sinai, New York, NY, USA

5 Amgen Inc., Thousand Oaks, CA, USA

6 Indiana University Purdue University Indianapolis, Indianapolis, IN, USA

7 Baylor College of Dentistry, TX A&M, Dallas, TX, USA

8 UCB Pharma, Slough, UK

9 Present Address: Radius Health, Inc., 950 Winter St, Waltham, MA 02451, USA

| | |
|---|---|
| MOI | Moment of inertia |
| FEA | Finite element analysis |
| BFR | Bone formation rate |
| MS/BS | Mineralizing surface/bone surface |
| DXA | Dual-energy X-ray absorptiometer |
| PFA | Paraformaldehyde |
| CFU-F | Colony-forming unit-fibroblastic |
| CFU-ob | Colony-forming unit-osteoblastic staining |
| MSC | Mesenchymal stem cells |
| TRAP | Tartrate-resistant acid phosphatase |
| H&E | Hematoxylin and eosin |
| CTX | Serum C-terminal telopeptide of Type I collagen |
| CTR | Calcitonin receptor |
| BV | Bone volume |
| TV | Tissue volume |
| Tb.N | Trabecular number |
| Tb.Th | Trabecular thickness |
| Tb.Sp | Trabecular separation |
| Conn.D | Connectivity density |
| SMI | Structure model index |
| OV | Osteoid volume |
| OS | Osteoid surface |
| N. Oc | Osteoclast number |
| Pm | Perimeter |

## Introduction

The decline in bone mass and deterioration of the skeletal architecture are well-known consequence of spinal cord injury (SCI). More than 50% of individuals with chronic SCI will sustain a low-impact or osteoporotic fracture at some point subsequent to being paralyzed [1]. At the sublesional long-bone epiphyses, bone loss rate may approach ~ 1% per week for the first year following injury [2]. The greatest decreases in bone mass and the most common sites for fragility fractures are observed at the distal femur and proximal tibia [2]. Fractures lead to serious medical complications including pressure ulcer formation, increased pain, spasticity, and lower limb amputation [3]. Despite these serious clinical complications, currently there is no standard or well-accepted guideline for the diagnosis, prevention, or treatment of SCI-induced osteoporosis.

Elucidation of the Wnt/β-catenin signaling pathway in bone homeostasis has transformed our understanding of the cellular and molecular mechanisms in bone formation and resorption [4–7]. Recent studies suggest that sclerostin is a key regulator of SCI-induced bone loss [8–12]. Encoded by the SOST gene, sclerostin is a glycoprotein secreted primarily by osteocytes under physiological conditions, and is a potent inhibitor of bone formation [13, 14]. Sclerostin binds to low-density lipoprotein receptor-related protein 5/6 and antagonizes the Wnt signaling pathway [15, 16]. Down-regulation of sclerostin is associated with increased osteogenesis and bone mass [17, 18]. Mechanical stimulation *in vivo* dramatically reduces the expression of sclerostin by osteocytes [19]. Moreover, targeted deletion of sclerostin in mice increased bone formation, bone mass and strength [17, 20], and these animals are resistant to unloading-induced bone loss [20]. In humans, mechanical unloading of bone occurs in various conditions that result in paralysis and the inability to ambulate. Therefore, the association between sclerostin and bone loss may be anticipated to be strongest in pathological conditions that result in individuals who occupy the lowest end of the activity spectrum, such as those with chronic SCI.

Recent studies conducted by our group and other investigators have shown that pharmacological inhibition of sclerostin with a sclerostin antibody (Scl-Ab), when administered immediately after lesion, prevents bone loss in animals with either acute motor-incomplete [11] or motor-complete SCI [10]. We have also reported that sclerostin-deficient mice are resistant to the major sublesional bone loss that invariably follows SCI [12]. However, other highly clinically relevant questions should be addressed, such as whether sclerostin inhibition is able to reverse bone loss in individuals with SCI who have been injured for several years and have had substantial sublesional bone loss, which represents the vast majority of the SCI population. Patients with SCI who are chronically immobilized are appreciated to develop several pathological changes that may contribute to the extensive loss of sublesional bone mass that occurs after SCI, including those of systemic hormonal, metabolic, and inflammatory disorders [10].

We hypothesize that Scl-Ab is able to reverse bone loss that has occurred after chronic motor-complete SCI. To test this hypothesis, an established rat model of sublesional bone loss following complete spinal cord transection [10, 21, 22] was used to investigate the effects on the sublesional skeleton after 8 weeks of treatment with Scl-Ab that was initiated 12 weeks after motor-complete SCI. Jin et al. reported that 4 weeks after SCI in rodents, the neural regenerative response has subsided, an astrocytic scar has been established at the injury site, and spontaneous functional recovery has reached a plateau, and, as such, has been characterized as a chronic model of SCI [23]. Other investigators have characterized 3–12 weeks after SCI in the rodent models as chronic injury [24–27]. We and others have demonstrated that motor-complete SCI resulted in dramatic decrease in trabecular bone mass (− 62 to − 76%) at the distal femur at 21–56 days post-injury [10, 28–31]. A reduction of trabecular bone mass by − 65% was observed 16 weeks after SCI in rodents, suggesting that bone loss sustains following the neurological injury [32]. Thus, initiating drug treatment after 12 weeks of SCI in a rodent model should represent a

sufficient duration of injury after which a substantial amount of bone loss will have occurred. In this study, the effects of Scl-Ab were examined on bone mass and architecture, histomorphometric indices of bone formation and resorption, osteoblastogenic and osteoclastogenic lineage of bone marrow progenitor cells, as well as gene expression associated with bone remolding.

## Materials and Methods

### Animals, Surgery, and Drug Administration

Eight-week-old male Wistar rats (275 g) were purchased from Charles River (Wilmington, MA, USA), housed in a temperature and humidity-controlled room providing a 12-h:12-h day:night cycle, and fed food and water *ad libitum*. All procedures were approved by the James J. Peters VA Medical Center Institutional Animal Care and Use Committee (IACUC). Spinal cord transection was performed, as previously described [10, 21, 22] and are described in more details in Supplemental Materials. Sham-transected animals received a laminectomy-only surgery (Sham animals, $n=10$). Twelve weeks following injury, a rat Scl-Ab (36.5 mg/ml, Amgen Inc., Thousand Oaks, California, USA) was subcutaneously administered at 25 mg/kg/week (SCI/Scl-Ab animals, $n=12$), or vehicle (saline; SCI animals, $n=11$),) and continued for 8 weeks. As used in our previous study [10], the half dose (25 mg/kg/week) of Scl-Ab relative to that (25 mg/kg/twice a week) in other studies [33–36] was chosen to use in the present study; the choice was based on Amgen's recommendation with a goal to explore the minimum effective dose of Scl-Ab capable of maintaining therapeutic efficacy at a lower cost (personal communication). For dynamic histomorphometric analysis, newly formed bone was labeled with fluorochromes by subcutaneous injection of calcein (10 mg/kg body weight) and xylenol orange (90 mg/kg body weight) on Day −6 and −2 before euthanasia, respectively. Eight weeks after Scl-Ab was started, animals were anesthetized by isoflurane inhalation. Additional details procedures for tissue collection are provided in Supplemental Materials.

### Bone Mineral Density, Structure, and Mechanical Properties

Areal bone mineral density (BMD) measurements were performed on all of the collected bone samples using a small animal dual-energy X-ray absorptiometer (DXA) (Lunar Piximus, Fitchburg, WI, USA), as previously described [10, 12, 21, 22, 37, 38]. Volumetric BMD and bone architecture of the distal femur and midshaft were assessed by a Scanco μCT scanner (μCT-40; Scanco Medical AG, Bassersdorf, Switzerland) at 16 mm isotropic voxel size, as previously described [10] and additional details may be found in Supplemental Materials.

Mechanical properties at the distal femur trabecular bones were estimated from micro-finite element analysis (μFEA), following the manufacturer's recommended procedures, as previously described [32, 39]. Briefly, μFEA models were produced by converting each bone voxel to an 8-node brick element. Bone tissue was subjected to applied uniaxial compression, with an elastic modulus of 15 GPa and Poisson's ratio of 0.3 for each element. A linear elastic analysis was used to estimate the bone stiffness and failure load.

### Bone Histomorphometric Studies

For fluorochrome-based determination of rates of bone formation by dynamic histomorphometry, 6-mm sections embedded in methyl methacrylate plastic were cut using a Reichert-Jung sledge microtome. Xylenol orange and calcein were visualized by fluorescent microscopy and the distance between labeled layers was used as a measure of the rate of bone formation, as determined by morphometry software. To quantify the osteoclast number, tartrate-resistant acid phosphatase (TRAP) staining was used to specifically label osteoclasts in deplasticized distal femur sections. Slides were counterstained with hematoxylin and eosin (H&E). Von Kossa/Tetrachrome staining was performed to measure osteoid volume and osteoid surface. Osteoclasts and osteoid were measured under bright field microscopy using an Olympus microscope with an OsteoMeasure system (Osteometrics, Atlanta, GA, USA). Additional details procedures performed are provided in Supplemental Materials.

### Serum Levels of CTX and Osteocalcin

Blood samples collected at termination were centrifuged at 1500 g for 10 min at 4 °C, and the serum was separated and then stored at − 80 °C. Serum C-terminal telopeptide of type I collagen (CTX) levels were measured using a RatLapsTM enzyme-immunoassay kit from Immunodiagnostic Systems (Fountain Hills, AZ). Serum concentrations of osteocalcin were measured using a rat osteocalcin immunoassay kit (Alfa Aesar). All samples were assayed in duplicate, following the manufacturer's recommended procedures, as previously described [22, 37].

### Ex Vivo Osteoblastogenesis and Osteoclastogenesis Assay

Procedures for osteoblast and osteoclast formation from bone marrow stem cells were performed, as previously described [10, 12, 21, 22, 37, 38] and are described in greater detail in Supplemental Materials.

### RNA Extraction and Quantitative PCR

Total RNAs were extracted from bone marrow cell cultures using the TRI reagent (Sigma-Aldrich). One µg of total RNA was used to synthesize the first strand cDNA by the High Capacity cDNA Reverse Transcription Kit (Applied Biosystems). Real-time PCR determination of mRNA levels was performed in the ViiA7 system (Applied Biosystems) as described previously [10, 12, 21, 22, 37, 38]. Relative expression levels were calculated using the $2^{-\Delta\Delta Ct}$ method with 18S RNA as an internal control [40].

### Statistics

Data are expressed as mean ± SEM. The number of independent samples ($n$) is provided in the legend of each figure. The statistical significance of differences among means was tested using one-way analysis of variance and a Newman–Keuls post hoc test to determine the significance of differences between individual pairs of means using a $p$ value of 0.05 as the cutoff for significance. Statistical calculations were performed using Prism 4.0c (GraphPad Software, La Jolla, CA, USA).

## Results

### Scl-Ab Restored BMD, Bone Structure, and Mechanical Strength in Rats After Chronic SCI

At the termination of the study, the animals had a ~ 50% gain in body weight, and there were no significant differences among Sham, SCI and SCI/Scl-Ab animal groups either before performing surgery or at time of sacrifice (Fig. 1A). At 20 weeks after SCI, BMD of distal femoral metaphysis, proximal tibial metaphysis, and the lumbar spine (L3–L5) were lower than those of the Sham animals by about − 22, − 15, and − 9%, respectively (Fig. 1B–D). Administration of Scl-Ab significantly increased the area BMD at the distal femur (+ 38.5%, $p < 0.001$; Fig. 1B), proximal tibia (+ 41.9%, $p < 0.001$; Fig. 1C), and lumbar spine (+ 47.7%, $p < 0.001$; Fig. 1D) when compared to SCI animals injected with vehicle. Notably, animals received Scl-Ab also showed higher BMD than control Sham animals at all three sites evaluated, with the greatest increase in BMD noted at the lumbar spine (+ 34.1%, $p < 0.001$; Fig. 1D).

Bone architecture was examined by high-resolution µCT to assess changes in trabecular bone of the distal femoral metaphysis (Fig. 2A). In vehicle-treated SCI animals, trabecular bone volume (BV/TV) at this site was significantly reduced (− 37.2%, $p < 0.001$; Fig. 2B-a), due largely to decreased trabecular number (Tb.N) (− 33%, $p < 0.001$; Fig. 2B-d) with no change in trabecular thickness (Tb.Th)

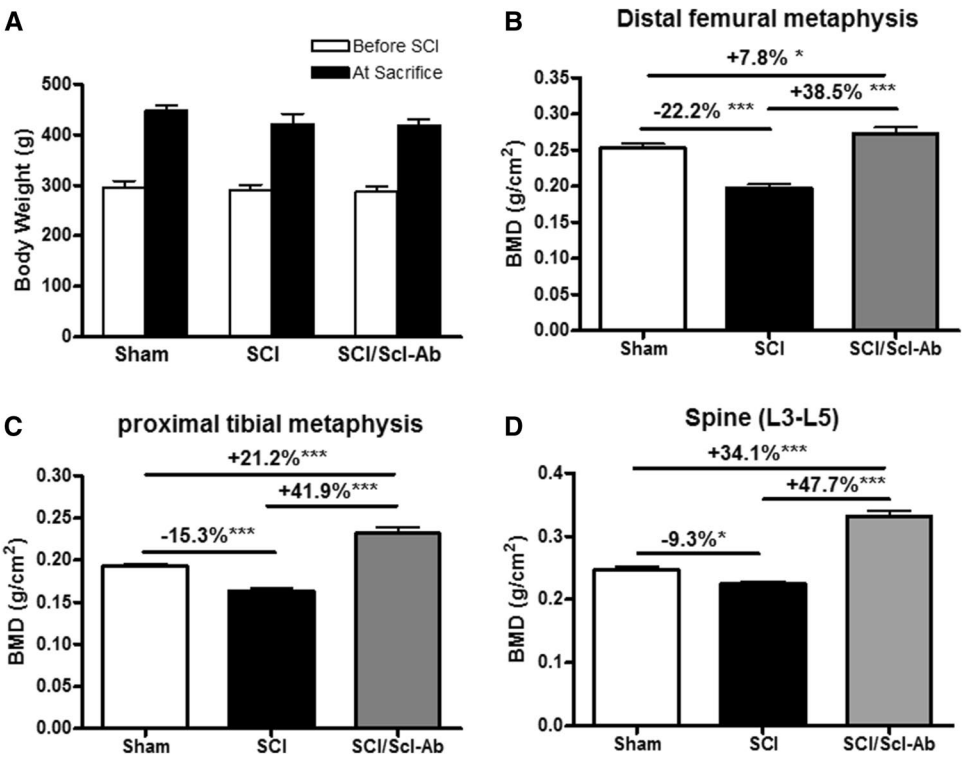


**Fig. 1** Sclerostin antibody reverses the loss in bone mineral density after chronic SCI. **A** Body weight before surgery and at sacrifice. Areal BMD acquired by DXA imaging at (**B**) distal femoral metaphysis, **C** proximal tibial metaphysis, and **D** lumbar spine. Data are expressed as Mean ± SEM, $^{*}p < 0.05$, $^{***}p < 0.001$ versus the indicated group by one-way ANOVA plus Newman–Keuls post hoc test, $n = 10$–12 animals per group

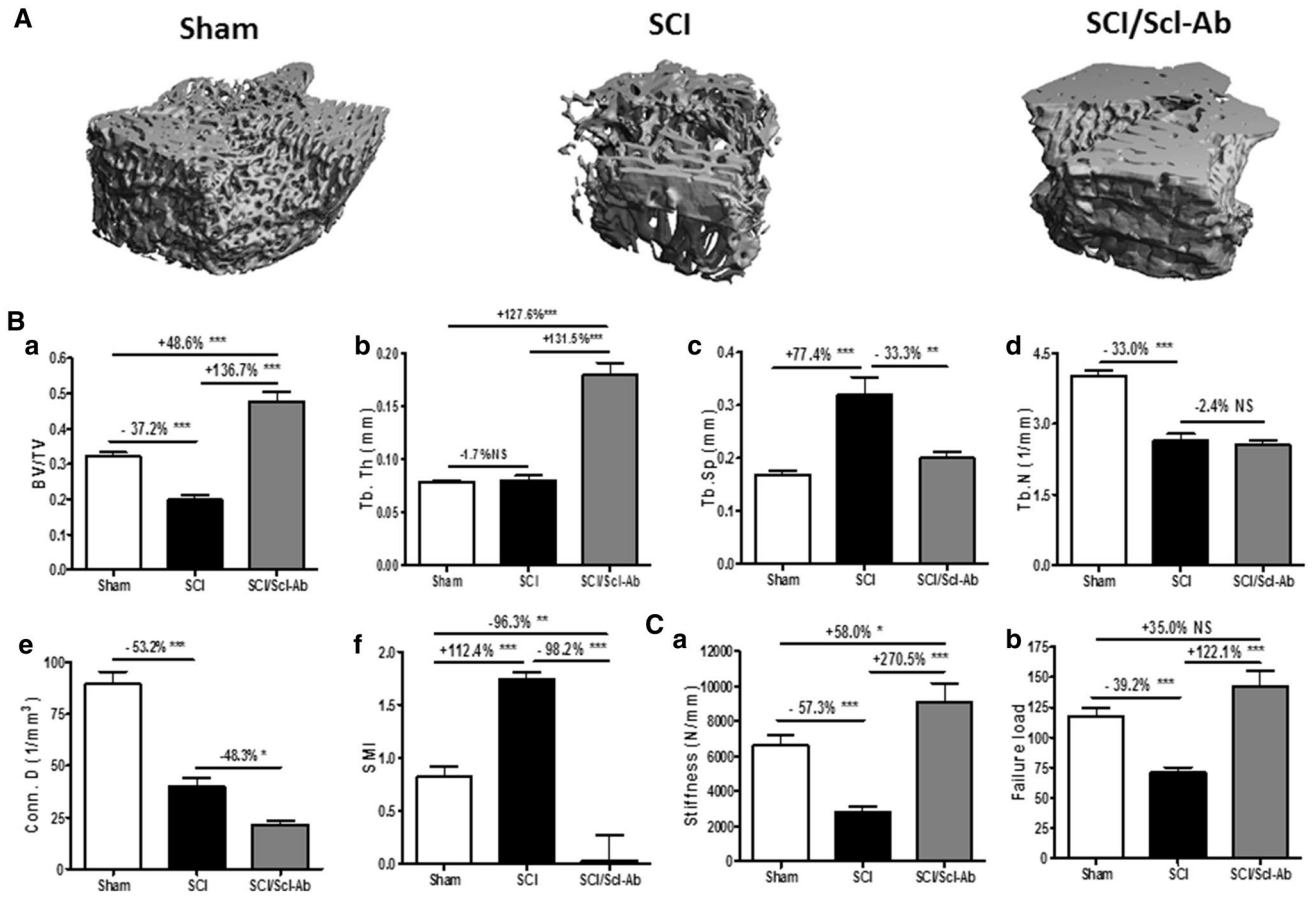


**Fig. 2** Effects of sclerostin antibody on trabecular bone architecture and strength in the trabecular distal femur metaphysis. **A** Representative μCT 3D images of trabecular microarchitecture. **B** Measurements are shown for (*a*) trabecular bone volume versus total bone volume (BV/TV, %); (*b*) trabecular thickness (Tb.Th, mm); (*c*) trabecular separation (Tb.Sp, mm); (*d*) trabecular number (Tb.N, $mm^{-1}$); (*e*) connectivity density (conn.D, $mm^{-3}$); and (*f*) structure model index (SMI, range from 0 to 3, with 0 = plate like and 3 = rod like). **C** Sclerostin antibody increases trabecular bone strength. (*a*) Bone stiffness and (*b*) failure load were estimated from micro-finite element analysis (μFEA). Data are expressed as Mean ± SEM, $*p<0.05$, $**p<0.01$, $***p<0.001$ versus the indicated group by one-way ANOVA plus Newman–Keuls post hoc test, $n = 10$–12 animals per group. *NS* not significant

(Fig. 2B-b). Trabecular connectivity was greatly reduced (Conn. D) (− 53.2%, $p<0.001$; Fig. 2B-e), associated with transformation from plate-like to rod-like structures as reflected by the higher structure model index (SMI) (+ 112.4%, $p<0.001$; Fig. 2B-f). Administration of Scl-Ab after SCI completely restored trabecular bone volume (+ 136.7%, $p<0.001$; Fig. 2B-a) and SMI, primarily by increasing trabecular thickness (+ 131.5%, $p<0.001$; Fig. 2B-b) and to a lesser degree, by decreasing trabecular separation (− 33.3%, $p<0.01$; Fig. 2B-c). Furthermore, administration of Scl-Ab to the SCI animals resulted in a far greater trabecular bone volume (Fig. 2B-a) and thickness (Fig. 2B-b), as well as a lower SMI (Fig. 2B-f), than those in the Sham animals.

Finite element analysis (FEA) based on μCT images was performed to evaluate the effect of Scl-Ab on bone mechanical strength. In vehicle-treated SCI animals, the bone stiffness was reduced by − 57.3% ($p<0.001$, Fig. 2C-a), and estimated failure load was reduced by − 39.2% ($p<0.001$, Fig. 2C-b). Scl-Ab treatment led to a drastic increase of estimated stiffness (+ 270.5% vs. SCI-vehicle and + 58.0% vs. sham; Fig. 2C-a) and failure load (+ 122.1% vs. SCI-vehicle, $p<0.001$; Fig. 2C-b). There is no difference in bone tissue vBMD across Sham, SCI, and SCI/Scl-Ab animal groups, suggesting that the changes in the estimated mechanical properties are specific, but not attributed to changes in material properties of the bone (Supplemental Fig. 1A).

Cortical bone structure at the femur midshaft was examined by high-resolution μCT (Fig. 3A). Cortical BMD was not significantly different at 20 weeks after SCI (Supplemental Fig. 1B). However, compared to those from the sham group, bones from the SCI group were thinner with reductions in bone area (− 15.3%, $p<0.05$; Fig. 3B-a) and total tissue area (− 16.7%, $p<0.05$; Fig. 3B-a) and a slight increase in endosteal perimeter (+ 1.3%; Fig. 3B-b), resulting in a − 7.6% decrease in cortical thickness (Ct. Th) ($p<0.01$;

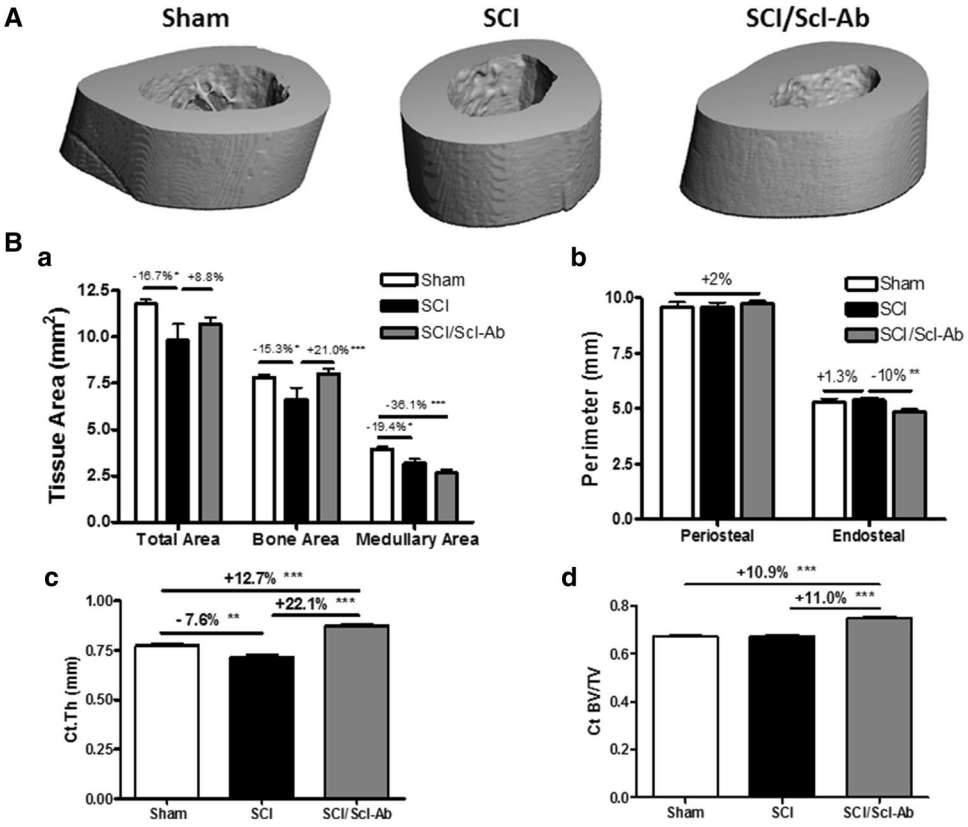


**Fig. 3** Effects of sclerostin antibody on cortical architecture of the femur midshaft. **A** Representative μCT 3D images of cortical microarchitecture are displayed. **B** Measurements are shown for (*a*) total, bone, and medullary tissue area ($mm^2$); (*b*) periosteal and endosteal perimeters (mm); (*c*) cortical thickness (Ct. Th, mm); (*d*) cortical bone volume over total tissue volume (Ct. BV/TV). Data are expressed as Mean ± SEM, $*p < 0.05$, $**p < 0.01$, $***p < 0.001$ versus the indicated group by one-way ANOVA plus Newman–Keuls post hoc test, $n = 10–12$ animals per group

Fig. 3B-c.). In Scl-Ab-treated SCI animals, a significant increase in both cortical bone volume (~ + 11% vs. SCI or Sham; Fig. 3B-d) and thickness (+ 22% vs. SCI-vehicle and + 12.7% vs. Sham; Fig. 3B-c) was observed. These sclerostin antibody-mediated changes are predominantly attributed to significant reductions in endosteal perimeter (− 10% vs. SCI-vehicle, $p < 0.01$; Fig. 3B-b) and medullary area (− 36.1% vs. sham, $p < 0.001$; Fig. 3B-a) and a moderate increase in periosteal perimeter (+ 2% vs. sham; Fig. 3B-b).

## Scl-Ab Greatly Enhanced Bone Formation in Rats After Chronic SCI

Serum osteocalcin level was slightly suppressed in vehicle-treated SCI animals, which was significantly elevated by Scl-Ab administration to the SCI animals (+ 23.1%, $p < 0.05$; Fig. 4A) compared to that in Sham animals. No significant difference in serum CTX levels were observed among Sham, SCI, and SCI/Scl-Ab animals (Supplemental Fig. 2A).

In parallel, dynamic histomorphometric analysis was performed to examine the effect of Scl-Ab on bone formation (Fig. 4B) at the distal femur. Although no decrease in bone formation rate (BFR/BS) or mineralizing surface (MS/BS) was detected in vehicle-treated SCI animals, increased new bone formation at the trabecular surface was present in Scl-Ab-treated animals, as evident by robust increases in BFR/BS ($p < 0.001$) and MS/BS ($p < 0.001$) (Fig. 4C).

Von Kossa/Tetrachrome staining was performed to measure osteoid volume (OV/TV or OV/BV) and osteoid surface (OS/BS). A marginal decrease in OV/TV or OV/BV and OS/BS was found in the vehicle-treated SCI animals compared to those in Sham animals (Fig. 5A). Scl-Ab administration in SCI animals resulted in substantial elevations in both osteoid volume (> 3.6 fold for OV/TV and > 7.4 fold for OV/BV, Fig. 5B) and osteoid surface (> 4.6 fold, Fig. 5B) to levels higher than those in Sham animals.

As our group has previously reported in animals after acute SCI [10], a significant reduction of osteoclast number (N. Oc/T. Ar and N. Oc/B. Pm) and surface (Oc. S/BS) at trabecular bone was observed in vehicle-treated SCI animals, when compared with Sham animals. Treatment with Scl-Ab in SCI animals did not significantly affect the osteoclast number (Supplemental Fig. 2B and 2C).

## Scl-Ab Increased Osteoblastogenesis and Inhibited Osteoclastogenesis in Bone Marrow Precursors in Rats After Chronic SCI

Colony-forming unit–fibroblastic (CFU-F) staining, a marker for commitment of bone marrow precursors to osteoblast lineage, was performed to evaluate the effect of

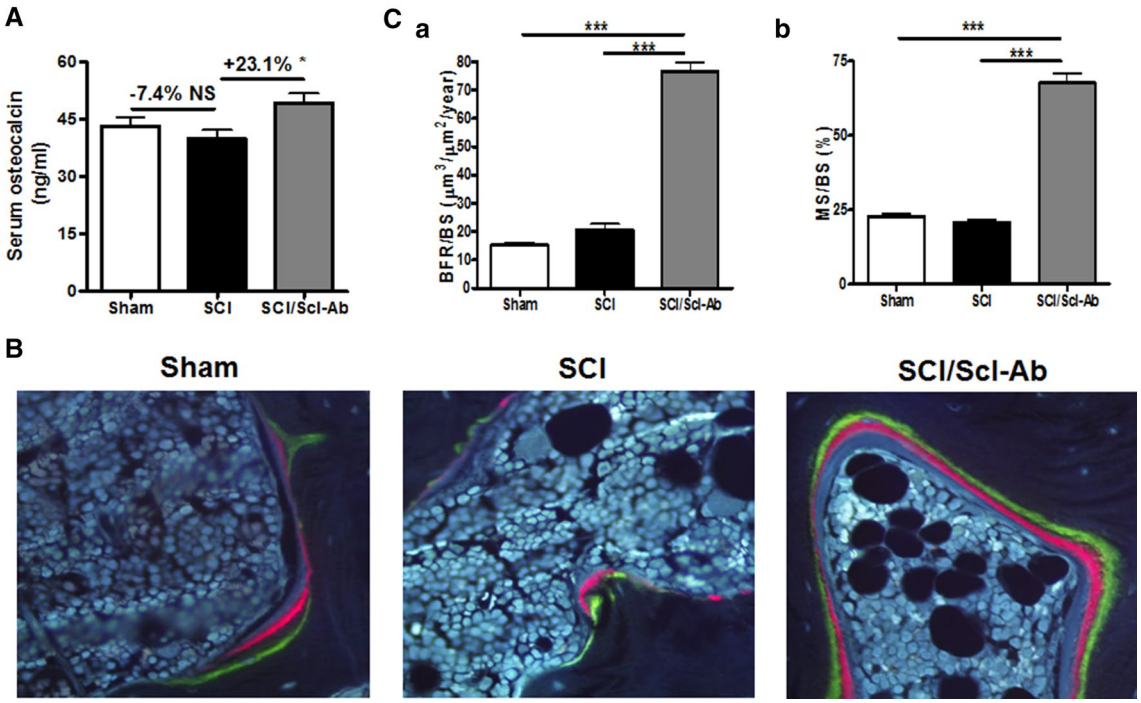


**Fig. 4** Sclerostin antibody increases bone formation of trabecular bone at the distal femur. **A** Bone formation marker osteocalcin levels were measured by ELISA. **B** Representative images of 6-µm-thick bone specimens showing double labeling of calcein green and xylenol orange under fluorescence microscopy (magnification ×20). **C** Measurement of (*a*) bone formation rate over bone surface (BFR/BS); and (*b*) mineralizing surface/bone surface (MS/BS). Data are expressed as Mean ± SEM, $^{**}p < 0.01$, $^{***}p < 0.001$ versus the indicated group by one-way ANOVA plus Newman–Keuls post hoc test, $n = 10$–12 animals per group. *NS* not significant

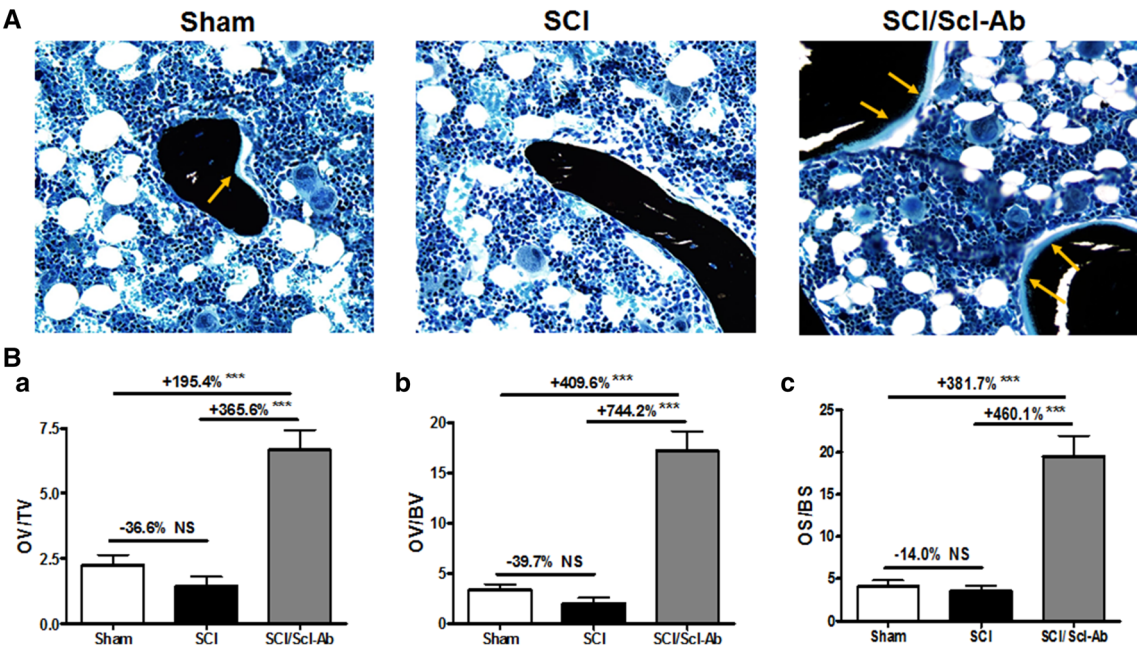


**Fig. 5** Effects of sclerostin antibody on osteoid volume and surface area at trabecular bone of distal femur. **A** Representative images of trabecular bone sections from the femoral metaphysis by Von Kossa/Tetrachrome staining (magnification ×20). The light blue area of VKM staining on trabecular surfaces representing osteoid is indicated by arrows. **B** (*a*) Histomorphometric quantification of osteoid volume versus total volume (OV/TV), (*b*) osteoid volume versus bone volume (OV/BV), and (*c*) osteoid surface versus bone surface (OS/BS). Data are expressed as Mean ± SEM, $^{***}p < 0.001$ versus the indicated group by one-way ANOVA plus Newman–Keuls post hoc test, $n = 10$–12 animals per group. *NS* not significant

Scl-Ab on osteoblastogenesis. At 20 weeks after SCI, the number of marrow stromal cells that stained positive for alkaline phosphatase was significantly reduced (Fig. 6A, B). Similarly, the values for mineralized nodules (CFU-osteoblastic [ob] staining) were significantly reduced in the vehicle-treated SCI group. Treatment with Scl-Ab in the SCI animals completely reversed these unfavorable changes (Fig. 6A, B). In *ex vivo* cultures of osteoblasts derived from bone marrow stromal precursors, although mRNA levels for the differentiation marker Runx2 and bone sialoprotein (BSP) did not significantly change (Supplemental Fig. 3A and B), the Wnt/β-catenin–responsive genes Tcf7 and ENC1 were reduced by − 30.1 and − 36.6%, while SOST (Fig. 6C) and sFRP1,2 mRNAs (Supplemental Fig. 3C and D) were significantly increased in the SCI group compared with the Sham group. Scl-Ab administration to the SCI group increased BSP, Tcf7, and ENC1 mRNA expression and decreased SOST and sFRP1,2 mRNA expression to levels comparable to those observed in Sham animals. SCI also resulted in a marginal decrease of OPG/RANKL ratio (− 15.7% vs. sham; Fig. 6C), which was completely reversed by administration of Scl-Ab (+ 66.0% vs. SCI, $p < 0.05$; Fig. 6C) to a level even higher than that observed in Sham animals.

An osteoclastogenesis assay using bone marrow hematopoietic precursors derived from femurs and tibias revealed an increase in $TRAP^+$ multinucleated cells in cultures of bone marrow cells from the vehicle-treated SCI rats, compared to those from Sham rats (Fig. 6D, E). The administration of Scl-Ab in animals with the SCI significantly reduced the number of $TRAP^+$ multinucleated cells ($p < 0.001$; Fig. 6D, E). In *ex vivo* cultures of osteoclasts derived from marrow hematopoietic precursors, levels for transcripts encoding the osteoclast differentiation markers TRAP and calcitonin receptor (CTR) were both increased in the SCI group compared with the Sham group (Fig. 6F). Scl-Ab treatment reduced the expression of TRAP mRNA to levels similar or below those detected in Sham animals (Fig. 6F).

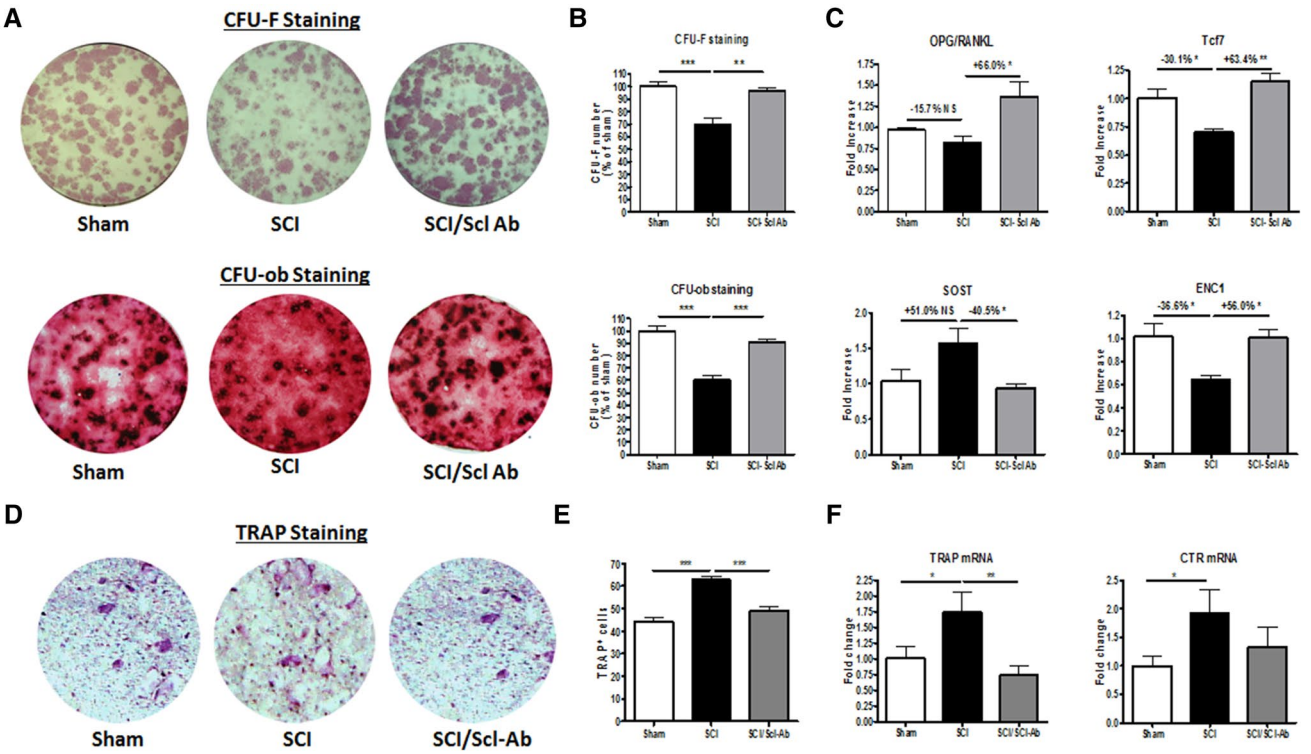


**Fig. 6** Sclerostin antibody promotes osteoblastogenesis and Inhibits osteoclastogenesis in bone marrow precursors in rats after chronic SCI. **A** Representative images showing alkaline phosphatase staining (CFU-F) and Von Kossa staining (CFU-ob) of cultured bone marrow stromal cells. **B** Quantification of $CFU\text{-}F^+$ cells and formed bone nodules. **C** Changes in gene expression of bone formation markers and Wnt signaling-related genes Tcf7, ENC1, OPG/RANKL ratio, and SOST in cultured bone marrow stromal cells. mRNA levels were determined by quantitative PCR. **D** Representative images showing the TRAP staining of cultured bone marrow stromal cells. **E** Quantification of $TRAP^+$ cells. **F** Changes in the gene expression of bone resorption markers TRAP and calcitonin receptor (CTR) in cultured bone marrow hematopoietic stem cells. mRNA levels were determined by quantitative PCR. Data are expressed as Mean ± SEM, $^*p < 0.05$, $^{**}p < 0.01$, $^{***}p < 0.001$ versus the indicated group by one-way ANOVA plus Newman–Keuls post hoc test, $n = 5$–6 animals per group; for each animal, three experimental replicates have been conducted

## Discussion

A recent clinical study in men with varying degrees of SCI found that sclerostin levels were highest in subjects who were injured less than 5 years [41], suggesting that the rapid bone loss early after paralysis due to motor-complete SCI could be attributed, at least in part, to elevated sclerostin levels, and that blocking sclerostin activity could be considered as a therapeutic option for patients with acute/subacute SCI. This hypothesis is supported by recent preclinical studies from our group and others, in which Scl-Ab prevented sublesional bone loss in rat models of acute SCI [10, 11]. However, our current knowledge concerning the role that sclerostin antagonism might play in the treatment of bone loss after chronic SCI has been essentially nonexistent. Morse et al. reported lower serum sclerostin levels and a strong positive correlation between serum sclerostin levels and BMD values in patients who had SCI for longer than 6 months, perhaps suggesting that sclerostin may not be an appropriate therapeutic target in the chronic SCI population [8], or more likely indicating that levels of sclerostin under steady-state conditions may serve as a marker for total skeletal mass. In contrast to the report by Morse et al. [8], a recent study by Invernizzi et al. demonstrated significantly higher values of serum sclerostin in chronic SCI (8 years after injury on average) compared to those in with healthy subjects [42].

The recent preclinical investigations suggest that the marked bone loss occurs a few weeks after injury and sustains in animal models of SCI [10, 29–32]. To our knowledge, the present study has provided the first direct preclinical evidence to demonstrate that Scl-Ab which is begun 12 weeks after motor-complete SCI largely reversed the cancellous bone loss, albeit the bone architecture was only partially restored. The restoration of bone mass and structure with Scl-Ab administration is associated with dramatically increased osteoblast activity, elevated bone formation rate, and increased osteoid indices. Specifically, robust cancellous bone deficits at the distal femur and the proximal tibia after 20 weeks of injury were observed. These deleterious microarchitecture changes were characterized by increased Tb.Sp, as well as reduced Tb.N, Conn.D, and plate-like geometry (SMI), indicative of compromised structural integrity and abridged mechanical strength. Pharmacological antagonism of sclerostin revealed bone anabolic effects that almost completely rescued the SCI-induced trabecular bone deterioration. These observations are consistent with benefits of Scl-Ab treatment that have been demonstrated in other rodent studies that have employed various approaches to mechanical unloading [43–45]. The administration of Scl-Ab to the animals after SCI resulted in changes to the trabecular bone microstructure (e.g., volume, thickness, and SMI) and parameters of bone formation (e.g., BFR, MS, and osteoid) that were significantly greater than those of the Sham animals. These treatment-induced supra-normal changes to the skeleton are most likely secondary to a dose effect; therefore, additional study should be considered to identify the minimum effective dose of Scl-Ab to maintain therapeutic efficacy.

A previous study in a rat model of acute motor-incomplete SCI reported no change in the cortical area and thickness [11]. Interestingly, in our more chronic motor-complete SCI model, significantly reduced bone tissue area and cortical thickness were detected, which is expected to contribute to the reduction in cortical bone stiffness and strength, a possibility that remains to be further addressed by additional biomechanical testing. Of note, administration of Scl-Ab not only significantly reduced endosteal perimeter and medullary area and increased cortical bone thickness, but also increased trabecular bone stiffness and the estimated failure load. Whether the benefits of Scl-Ab demonstrated in this study could be translated to patients with SCI to reduce fracture occurrence at the sublesional skeletal sites remains to be determined in the future.

We previously reported that the reduced bone formation was observed in rats with acute motor-complete SCI by dynamic bone histomorphometry analysis and that Scl-Ab administration prevented the decrease in the bone formation rate [10]. In this study, although no change of bone formation rate or mineral surface was detected in animals that had more prolonged SCI prior to initiating therapy, pharmacological inhibition of sclerostin resulted in an about sevenfold elevation of both bone formation rate and mineralizing surface. In addition, more prolonged SCI led to a marginal decrease of osteoid volume and osteoid surface, whereas Scl-Ab treatment to the SCI animals increased the osteoid formation to levels even higher than those observed in Sham-operated animals. This histomorphometric finding is in an agreement with our ELISA results in which a marginal decrease of serum osteocalcin level was detected in rats after prolonged SCI and that Scl-Ab administration to the SCI rats significantly increased the serum osteocalcin level. These data are in contrast to the finding from a previous report in which serum osteocalcin was not elevated by Scl-Ab treatment, whereas P1NP (a circulating marker of type I collagen deposition) was reduced by SCI, an effect that was completely prevented by Scl-Ab [11].

Furthermore, analogous to our previous findings in animals with acute SCI [10], Scl-Ab favorably altered the differentiation potential of bone marrow progenitors by enhancing osteoblastogenesis and inhibiting osteoclastogenesis in animals with more prolonged SCI. These findings are consistent with a recent report that showed that Scl-Ab reversed unloading-induced reduction of marrow stromal cells colony

numbers, alkaline phosphatase-positive osteoblasts, and bone nodules [43]. The promotion of osteoblastogenesis and the inhibition of osteoclastic genes are consistent with altered expression Wnt signaling pathway genes, including the elevated expression of Tcf7, ENC1, and the OPG/RANKL ratio, as well as reduced expression of RANKL and sFRP1,2. It is noted that recent findings support a relationship between greater Wnt signaling, increased *Enc1* expression, and improved osteoblast differentiation [21, 22]. In this study, no change in level of serum sclerostin was noted after more prolonged SCI (data not shown) when compared to that of Sham-operated animals. Of interest, levels of SOST expression in bone marrow-derived osteoblasts was up-regulated after chronic SCI in our study, which is consistent with the reported finding in patients with chronic SCI of elevated sclerostin levels associated with bone loss [42], and the change was reversed by Scl-Ab treatment. Appreciating that bone marrow cells compose a component of the local bone microenvironment, the increased level of SOST mRNA expression in bone marrow cells is a more physiologically meaningful finding and indicative of the role that sclerostin plays in the adaptation of the skeleton after SCI than that of alterations in circulating levels of sclerostin. Repeat dosing of Scl-Ab has shown to up-regulate Wnt antagonists, including sclerostin and Dkk1 in bone tissues of animal models, which results in a negative feedback response to limit canonical Wnt signaling [46–48]. We previously reported that sclerostin antibody increased the number of osteocytes; therefore, it is not unexpected that sclerostin antibody would result in increased SOST expression in the bone tissue since sclerostin is produced mainly by osteocytes and the appearance of additional osteocytes should produce greater levels of sclerostin. Taken together, the overall effect on gene expression of Scl-Ab in local marrow microenvironment has a unique role to activate the Wnt signaling pathway in mesenchymal stem cells (MSCs), thereby facilitating the recruitment of MSCs into the osteoblast cell lineage.

In summary, when initiated 12 weeks after SCI and continued for 8 weeks in a rat model of motor-complete SCI, administration of sclerostin-neutralizing antibody resulted in a dramatic increase in bone formation and bone mass in the skeleton below the spinal cord lesion. The mechanisms underlying the observed anabolic activities of Scl-Ab are its normalization of osteoblastogenic and osteoclastogenic potential of bone marrow progenitors that were unfavorably impaired after SCI. Although SCI leads to rapid bone loss and high fracture incidence, there are currently no widely accepted clinical guidelines to address the consequences of bone loss in individuals after chronic SCI. Bisphosphonate administration has not been consistently reported to reverse sublesional bone loss in individuals after chronic SCI [1, 49]. Thus, our current preclinical findings provide a strong rationale to initiate clinical trials to evaluate the effectiveness of sclerostin antibody immunotherapy as a means to reverse bone loss in individuals with chronic SCI, in addition to its potential role in the prevention of bone loss shortly following acute SCI, as has been previously reported in our preclinical work [10].

**Acknowledgements** This work was supported by the Veterans Health Administration, Rehabilitation Research and Development Service (Grants 5I01RX001313, 5I01RX02089-A2, and 5I01RX000687 to WQ; B9212-C and B2020-C to WAB). Amgen Inc. and UCB Pharma provided Scl-Ab.

**Author Contributions** WZ, XL, HK, WAB, and WQ were responsible for study design and data analysis. WZ, XL, YP, JP, JL, AX, YQ, JF, and CPC conducted the study. The manuscript was written by WZ and WQ and was revised and approved by all authors. WQ takes responsibility for the integrity of the data analysis.

## Compliance with Ethical Standards

**Conflict of interest** Wei Zhao, Yuanzhen Peng, Yiwen Qin, Jianping Pan, Jiliang Li, Aihua Xu, Jian Q. Feng, William A. Bauman, Christopher Cardozo, and Weiping Qin declare that they have no conflict of interest. XL is current employee and shareholder of Amgen Inc. MSO is an ex-Amgen employee and owns Amgen stocks, and HZK is current employee of UCB Pharma and shareholder of UCB Pharma and Amgen.

**Human and Animal Rights and Informed Consent** All applicable international, national, and institutional guidelines for the care and use of animals were followed.

## References

1. Bauman WA, Cardozo CP (2015) Osteoporosis in individuals with spinal cord injury. PM R 7(2):188–201. https://doi.org/10.1016/j.pmrj.2014.08.948
2. Qin W, Bauman WA, Cardozo C (2010) Bone and muscle loss after spinal cord injury: organ interactions. Ann N Y Acad Sci 1211:66–84. https://doi.org/10.1111/j.1749-6632.2010.05806.x
3. Morse LR, Battaglino RA, Stolzmann KL, Hallett LD, Waddimba A, Gagnon D et al (2009) Osteoporotic fractures and hospitalization risk in chronic spinal cord injury. Osteoporos Int 20(3):385–92. https://doi.org/10.1007/s00198-008-0671-6
4. Bonewald LF, Johnson ML (2008) Osteocytes, mechanosensing and Wnt signaling. Bone 42(4):606–615. https://doi.org/10.1016/j.bone.2007.12.224
5. Glass DA, Bialek P, Ahn JD, Starbuck M, Patel MS, Clevers H et al (2005) Canonical Wnt signaling in differentiated osteoblasts controls osteoclast differentiation. Dev Cell 8(5):751–64. https://doi.org/10.1016/j.devcel.2005.02.017
6. Manolagas SC (2014) Wnt signaling and osteoporosis. Maturitas 78(3):233–237. https://doi.org/10.1016/j.maturitas.2014.04.013
7. Zaidi M (2007) Skeletal remodeling in health and disease. Nat Med 13(7):791–801. https://doi.org/10.1038/nm1593
8. Morse LR, Sudhakar S, Danilack V, Tun C, Lazzari A, Gagnon DR et al (2012) Association between sclerostin and bone density in chronic spinal cord injury. J Bone Miner Res 27(2):352–359. https://doi.org/10.1002/jbmr.546

9. Morse LR, Sudhakar S, Lazzari AA, Tun C, Garshick E, Zafonte R et al (2013) Sclerostin: a candidate biomarker of SCI-induced osteoporosis. Osteoporos Int 24(3):961–968. https://doi.org/10.1007/s00198-012-2072-0
10. Qin W, Li X, Peng Y, Harlow LM, Ren Y, Wu Y et al (2015) Sclerostin antibody preserves the morphology and structure of osteocytes and blocks the severe skeletal deterioration after motor-complete spinal cord injury in rats. J Bone Miner Res 30(11):1994–2004. https://doi.org/10.1002/jbmr.2549
11. Beggs LA, Ye F, Ghosh P, Beck DT, Conover CF, Balaez A et al (2015) Sclerostin inhibition prevents spinal cord injury-induced cancellous bone loss. J Bone Miner Res 30(4):681–689. https://doi.org/10.1002/jbmr.2396
12. Qin W, Zhao W, Li X, Peng Y, Harlow LM, Li J et al (2016) Mice with sclerostin gene deletion are resistant to the severe sublesional bone loss induced by spinal cord injury. Osteoporos Int. https://doi.org/10.1007/s00198-016-3700-x
13. Balemans W, Ebeling M, Patel N, Van Hul E, Olson P, Dioszegi M et al (2001) Increased bone density in sclerosteosis is due to the deficiency of a novel secreted protein (SOST). Hum Mol Genet 10(5):537–43
14. Staehling-Hampton K, Proll S, Paeper BW, Zhao L, Charmley P, Brown A et al (2002) A 52-kb deletion in the SOST-MEOX1 intergenic region on 17q12-q21 is associated with van Buchem disease in the Dutch population. Am J Med Genet 110(2):144–52. https://doi.org/10.1002/ajmg.10401
15. Semenov M, Tamai K, He X (2005) SOST is a ligand for LRP5/LRP6 and a Wnt signaling inhibitor. J Biol Chem 280(29):26770–26775. https://doi.org/10.1074/jbc.M504308200
16. Semenov MV, He X (2006) LRP5 mutations linked to high bone mass diseases cause reduced LRP5 binding and inhibition by SOST. J Biol Chem 281(50):38276–38284. https://doi.org/10.1074/jbc.M609509200
17. Li X, Ominsky MS, Niu QT, Sun N, Daugherty B, D'Agostin D et al (2008) Targeted deletion of the sclerostin gene in mice results in increased bone formation and bone strength. J Bone Miner Res 23(6):860–869. https://doi.org/10.1359/jbmr.080216
18. MacDonald BT, Joiner DM, Oyserman SM, Sharma P, Goldstein SA, He X et al (2007) Bone mass is inversely proportional to Dkk1 levels in mice. Bone 41(3):331–339. https://doi.org/10.1016/j.bone.2007.05.009
19. Robling AG, Niziolek PJ, Baldridge LA, Condon KW, Allen MR, Alam I et al (2008) Mechanical stimulation of bone in vivo reduces osteocyte expression of Sost/sclerostin. J Biol Chem 283(9):5866–5875. https://doi.org/10.1074/jbc.M705092200
20. Lin C, Jiang X, Dai Z, Guo X, Weng T, Wang J et al (2009) Sclerostin mediates bone response to mechanical unloading through antagonizing Wnt/beta-catenin signaling. J Bone Miner Res 24(10):1651–1661. https://doi.org/10.1359/jbmr.090411
21. Sun L, Pan J, Peng Y, Wu Y, Li J, Liu X et al (2013) Anabolic steroids reduce spinal cord injury-related bone loss in rats associated with increased Wnt signaling. J Spinal Cord Med 36(6):616–22. https://doi.org/10.1179/2045772312Y.0000000020
22. Qin W, Sun L, Cao J, Peng Y, Collier L, Wu Y et al (2013) The central nervous system (CNS)-independent anti-bone-resorptive activity of muscle contraction and the underlying molecular and cellular signatures. J Biol Chem 288(19):13511–13521. https://doi.org/10.1074/jbc.M113.454892
23. Jin Y, Fischer I, Tessler A, Houle JD (2002) Transplants of fibroblasts genetically modified to express BDNF promote axonal regeneration from supraspinal neurons following chronic spinal cord injury. Exp Neurol 177(1):265–75
24. Schallert T, Fleming SM, Leasure JL, Tillerson JL, Bland ST (2000) CNS plasticity and assessment of forelimb sensorimotor outcome in unilateral rat models of stroke, cortical ablation, parkinsonism and spinal cord injury. Neuropharmacology 39(5):777–87
25. Fischer FR, Peduzzi JD (2007) Functional recovery in rats with chronic spinal cord injuries after exposure to an enriched environment. J Spinal Cord Med 30(2):147–55
26. Wang X, Duffy P, McGee AW, Hasan O, Gould G, Tu N et al (2011) Recovery from chronic spinal cord contusion after Nogo receptor intervention. Ann Neurol 70(5):805–21. https://doi.org/10.1002/ana.22527
27. Hesp ZC, Goldstein EZ, Miranda CJ, Kaspar BK, McTigue DM (2015) Chronic oligodendrogenesis and remyelination after spinal cord injury in mice and rats. J Neurosci 35(3):1274–1290. https://doi.org/10.1523/JNEUROSCI.2568-14.2015
28. Ruth EB. Metamorphosis of the pubic symphysis. I. The white rat (Mus norvegicus albinus). Anat Rec. 1935;(64):1–7
29. Voor MJ, Brown EH, Xu Q, Waddell SW, Burden RL, Burke DA et al (2011) Bone loss following spinal cord injury in a rat model. J Neurotrauma. https://doi.org/10.1089/neu.2011.2037
30. Minematsu A, Nishii Y, Imagita H, Sakata S (2014) Time course of changes in trabecular bone microstructure in rats with spinal cord injury. J Life Sci. 8(6):522–528
31. Zamarioli A, Battaglino RA, Morse LR, Sudhakar S, Maranho DA, Okubo R et al (2013) Standing frame and electrical stimulation therapies partially preserve bone strength in a rodent model of acute spinal cord injury. Am J Phys Med Rehabil 92(5):402–10. https://doi.org/10.1097/PHM.0b013e318287697c
32. Lin T, Tong W, Chandra A, Hsu SY, Jia H, Zhu J et al (2015) A comprehensive study of long-term skeletal changes after spinal cord injury in adult rats. Bone Res 3:15028. https://doi.org/10.1038/boneres.2015.28
33. Ren Y, Han X, Ho SP, Harris SE, Cao Z, Economides AN et al (2015) Removal of SOST or blocking its product sclerostin rescues defects in the periodontitis mouse model. FASEB J 29(7):2702–2711. https://doi.org/10.1096/fj.14-265496
34. Li X, Ominsky MS, Warmington KS, Morony S, Gong J, Cao J et al (2009) Sclerostin antibody treatment increases bone formation, bone mass, and bone strength in a rat model of postmenopausal osteoporosis. J Bone Miner Res 24(4):578–588. https://doi.org/10.1359/jbmr.081206
35. Chen H, Xu X, Liu M, Zhang W, Ke HZ, Qin A et al (2015) Sclerostin antibody treatment causes greater alveolar crest height and bone mass in an ovariectomized rat model of localized periodontitis. Bone 76:141–148. https://doi.org/10.1016/j.bone.2015.04.002
36. Taut AD, Jin Q, Chung JH, Galindo-Moreno P, Yi ES, Sugai JV et al (2013) Sclerostin antibody stimulates bone regeneration after experimental periodontitis. J Bone Miner Res 28(11):2347–2356. https://doi.org/10.1002/jbmr.1984
37. Bramlett HM, Dietrich WD, Marcillo A, Mawhinney LJ, Furones-Alonso O, Bregy A et al (2014) Effects of low intensity vibration on bone and muscle in rats with spinal cord injury. Osteoporos Int 25(9):2209–2219. https://doi.org/10.1007/s00198-014-2748-8
38. Cardozo CP, Qin W, Peng Y, Liu X, Wu Y, Pan J et al (2010) Nandrolone slows hindlimb bone loss in a rat model of bone loss due to denervation. Ann N Y Acad Sci 1192:303–306. https://doi.org/10.1111/j.1749-6632.2009.05313.x
39. Pistoia W, van Rietbergen B, Lochmuller EM, Lill CA, Eckstein F, Ruegsegger P (2002) Estimation of distal radius failure load with micro-finite element analysis models based on three-dimensional peripheral quantitative computed tomography images. Bone 30(6):842–848
40. Livak KJ, Schmittgen TD (2001) Analysis of relative gene expression data using real-time quantitative PCR and the 2(-Delta Delta C(T)) method. Methods 25(4):402–408. https://doi.org/10.1006/meth.2001.1262

41. Battaglino RA, Sudhakar S, Lazzari AA, Garshick E, Zafonte R, Morse LR (2012) Circulating sclerostin is elevated in short-term and reduced in long-term SCI. Bone 51(3):600–605. https://doi.org/10.1016/j.bone.2012.04.019
42. Invernizzi M, Carda S, Rizzi M, Grana E, Squarzanti DF, Cisari C et al (2015) Evaluation of serum myostatin and sclerostin levels in chronic spinal cord injured patients. Spinal Cord 53(8):615–620. https://doi.org/10.1038/sc.2015.61
43. Shahnazari M, Wronski T, Chu V, Williams A, Leeper A, Stolina M et al (2012) Early response of bone marrow osteoprogenitors to skeletal unloading and sclerostin antibody. Calcif Tissue Int 91(1):50–58. https://doi.org/10.1007/s00223-012-9610-9
44. Spatz JM, Ellman R, Cloutier AM, Louis L, van Vliet M, Suva LJ et al (2013) Sclerostin antibody inhibits skeletal deterioration due to reduced mechanical loading. J Bone Miner Res 28(4):865–74. https://doi.org/10.1002/jbmr.1807
45. Tian X, Jee WS, Li X, Paszty C, Ke HZ (2011) Sclerostin antibody increases bone mass by stimulating bone formation and inhibiting bone resorption in a hindlimb-immobilization rat model. Bone 48(2):197–201. https://doi.org/10.1016/j.bone.2010.09.009
46. Holdsworth G, Greenslade K, Jose J, Stencel Z, Kirby H, Moore A et al (2018) Dampening of the bone formation response following repeat dosing with sclerostin antibody in mice is associated with up-regulation of Wnt antagonists. Bone 107:93–103. https://doi.org/10.1016/j.bone.2017.11.003
47. Taylor S, Ominsky MS, Hu R, Pacheco E, He YD, Brown DL et al (2016) Time-dependent cellular and transcriptional changes in the osteoblast lineage associated with sclerostin antibody treatment in ovariectomized rats. Bone 84:148–59. https://doi.org/10.1016/j.bone.2015.12.013
48. Florio M, Gunasekaran K, Stolina M, Li X, Liu L, Tipton B et al (2016) A bispecific antibody targeting sclerostin and DKK-1 promotes bone mass accrual and fracture repair. Nat Commun 7:11505. https://doi.org/10.1038/ncomms11505
49. Chang KV, Hung CY, Chen WS, Lai MS, Chien KL, Han DS (2013) Effectiveness of bisphosphonate analogues and functional electrical stimulation on attenuating post-injury osteoporosis in spinal cord injury patients- a systematic review and meta-analysis. PLoS ONE 8(11):e81124. https://doi.org/10.1371/journal.pone.0081124